The Effects of the Short QT Syndrome on Electrical and Mechanical Function of the Heart: Insights from Modelling

Ismail Adeniran[1], Jules C. Hancox[2], Henggui Zhang[1]

[1]University of Manchester, [2]University of Bristol

Correspondence: henggui.zhang@manchester.ac.uk 0044161 306 3966, Oxford Road, M13 9PL, UK

Introduction

The Short QT Syndrome (SQTS) is a recently identified genetic cardiac channelopathy. It is characterised by abnormally short QT intervals on the electrocardiogram (ECG) including altered T-wave morphology (tall and peaked T-waves), poor rate adaptation of the QT interval, an increased incidence of atrial and ventricular arrhythmias and an increased risk of sudden death (1–6). Currently, five distinct forms of the condition have been identified, three (gain-of-function mutations) of which affect different cardiac potassium (K^+) ion channels; *KCNH2* (SQT1), *KCNQ1* (SQT2), *KCNH2* (SQT3) with the last two (loss-of-function mutations) affecting the L-type calcium channel (I_{CaL}); *CACNA1C* (SQT4) and *CACNB2b* (SQT5).

There are currently no phenotypically accurate models of the SQTS and whilst, *in vitro* electrophysiology and echocardiography of SQT mutant channels provide a means for greater comprehension of the effects of the SQTS, this approach on its own is insufficient to explain how arrhythmias arise, are maintained and how the SQTS affects mechanical systole and diastole and vice-versa. *In silico* modelling provides a powerful and complementary alternative to elucidating the functional consequences of the SQTS both electrically and mechanically.

Methods and Results

In this study, we developed an electromechanical model of the human ventricular myocyte by coupling a human ventricular myocyte model for electrical activity (VM) (7) with the Rice myofilament mechanical model (MM) (8). The resulting electromechanical model was used to investigate the electromechanical consequences of SQT1, SQT2 and SQT3 at the single cell, 2D and 3D tissue levels.

The VM and MM models were coupled by using as input to the MM model, the cytosolic calcium concentration from the VM model. The effect of calcium binding with troponin from the MM model was added to the calcium concentration from the VM model, thus providing a feedback pathway between both models.

For SQT1, we used our biophysically-detailed Markov chain model (9), which incorporates the experimentally-observed kinetic properties of the N588K-mutated hERG/I_{Kr} channel. SQT2 was modelled by modifying the I_{Ks} Markov chain model formulation of Silva and Rudy (10) to reproduce the experimentally-observed kinetic properties of the V307L-mutated I_{Ks} channel. For SQT3, we used our Hodgkin-Huxley model (11), which also incorporates the experimentally-observed kinetic properties of the D172N-mutant $I_{Kir2.1}$.

Figure 1 shows an example single cell simulation result for SQT3 obtained using a standard S1-S2 pacing protocol with 100 conditioning pulses (S1) at 1 Hz and a final stimulus pulse (S2). Figure 1Ai-Ci shows the abbreviation of the action potential (AP) by the SQT3 mutation in the epicardial (EPI), mid-myocardial (MCELL) and endocardial (ENDO) cell types. It also reduces the peak calcium concentration by 14% in the EPI and ENDO cells and by 20% in the MCELL (Figure 2Aii-Cii). In wildtype (WT) EPI and ENDO cells, the sarcomere length (SL) contracts

from 2.17 μm to ~2.04 μm but only to 2.16 μm under the SQT3 mutation. In the WT MCELL, the SL contracts from 2.17 μm to 1.91 μm but only to 1.97 μm under the SQT3 mutation (Figure 1Aiii-Ciii). Consequently, the SQT3 mutation reduces the contraction force by 35% in the EPI and ENDO cells and by 20% in the MCELL (Figure 1Aiv-Civ).

SQT1 and SQT2 (data not shown) also abbreviated the AP in the EPI, MCELL and ENDO cell types. In the EPI and ENDO cells, peak calcium concentration was reduced by 36% (SQT1) and 34% (SQT2) and by 47% (SQT1) and 17% (SQT2) in the MCELL. In SQT1 WT, the SL contracts from 2.17 μm to ~2.02 μm (EPI), ~1.90 μm (MCELL) and ~2.05 μm (ENDO) but only to 2.15 μm under the SQT1 mutation. Consequently, the SQT1 mutation reduces the contractile force by 80%.

In SQT2 WT, the SL contracts from 2.17 μm to ~2.09 μm (EPI), ~1.95 μm (MCELL) and ~2.12 μm (ENDO). This is reduced with the SQT2 mutation to ~2.16 μm (EPI), ~2.01 μm (MCELL) and ~2.16 μm (ENDO). Consequently, the SQT2 mutation reduces the contractile force by 80% in the EPI and EBDO cells and by 27% in the MCELL.

As an example, Figure 2 shows SQT3 simulation results in an idealised, isotropic, transmural left ventricular 2D sheet measuring 15 mm by 50 mm. Along the x-axis, the first 3.75 mm (25%) consists of ENDO cells, the next 5.25 mm (35%) consists of MCELLs with the remainder being EPI cells. There are 100 cells along the base (x-axis) and 333 cells along the y-axis giving a spatial resolution of 0.15 mm. The 2D mechanics mesh is fixed at the four corners, to avoid rigid body rotation while the unrestricted edges are free to move and have no externally applied force. In a realistic setting, the four clamped corners would move in tandem with the ventricular geometry.

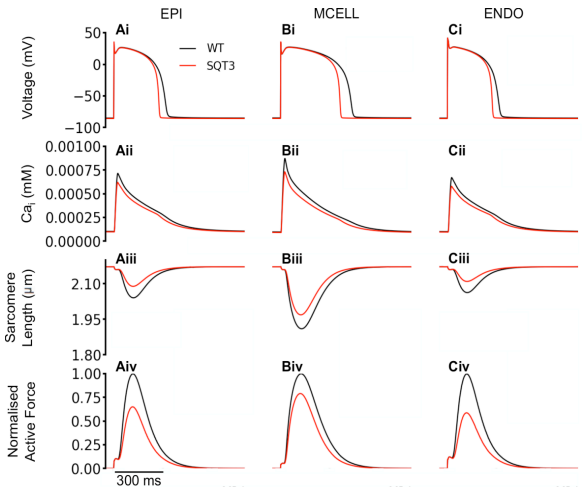

Figure 1: (Ai,Bi,Ci):WT (black) and SQT3 (red) action potentials in the EPI (Ai), MCELL (Bi) and ENDO (Ci) cells. **(Aii,Bii,Cii)**: WT (black) (black) and SQT3 (red) calcium concentration. **(Aiii,Biii,Ciii):** WT (black) and SQT3 (red) sarcomere length. **(Aiv,Biv,Civ):** WT (black) and SQT3 (red) normalised active force.

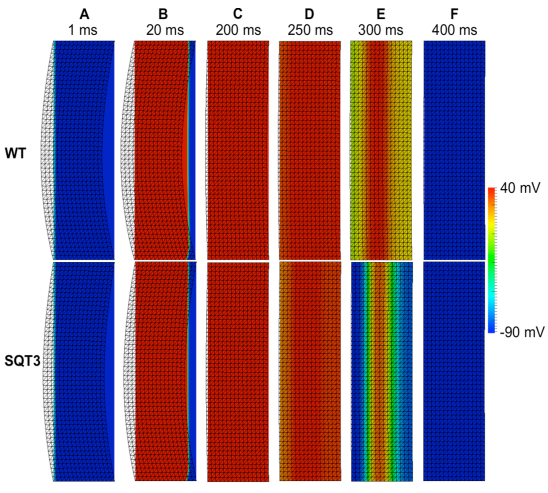

Figure 2: Electromechanical coupling in 2D ventricular tissue under the SQT3 mutation.
WT: Snapshots of tissue deformation induced by the superimposed electrical wave propagation in WT.
SQT3: Snapshots of tissue deformation induced by the superimposed electrical wave propagation.

Figure 2 shows the electrical wave propagation in the electrical mesh, on which is superimposed, the mechanics mesh (in wireframe) showing deformations induced by the active tension calculated from the electrical wave propagation at 10 ms, 20 ms, 200 ms, 250 ms, 300 ms and 300 ms.

Conclusions and Discussion

We have developed a human electromechanical model for ventricular myocytes and used it to investigate the functional consequences of the SQTS on ventricular contraction at single cell, 2D tissue and 3D organ levels. The example SQT3 simulation results show that the mutation compromises the binding of calcium to troponin leading to impaired interaction between actin and myosin and thereby less ventricular contractile force.

References

1. Gaita F, Giustetto C, Bianchi F, Wolpert C, Schimpf R, Riccardi R, et al. Short QT Syndrome: a familial cause of sudden death. Circulation. 2003 Aug 26;108(8):965–70.

2. Giustetto C, Di Monte F, Wolpert C, Borggrefe M, Schimpf R, Sbragia P, et al. Short QT syndrome: clinical findings and diagnostic-therapeutic implications. Eur. Heart J. 2006 Oct;27(20):2440–7.

3. Schimpf R, Wolpert C, Gaita F, Giustetto C, Borggrefe M. Short QT syndrome. Cardiovasc. Res. 2005 Aug 15;67(3):357–66.

4. Anttonen O, Junttila J, Giustetto C, Gaita F, Linna E, Karsikas M, et al. T-Wave morphology in short QT syndrome. Ann Noninvasive Electrocardiol. 2009 Jul;14(3):262–7.

5. McPate MJ, Witchel HJ, Hancox JC. Short QT syndrome. Future Cardiol. 2006 May;2(3):293–301.

6. Hancox JC, McPate MJ, Harchi A, Duncan RS, Dempsey CE, Witchel HJ, et al. The Short QT Syndrome. In: Tripathi ON, Ravens U, Sanguinetti MC, editors. Heart Rate and Rhythm [Internet]. Berlin, Heidelberg: Springer Berlin Heidelberg; 2011 [cited 2011 Jul 10]. p. 431–49. Available from: http://www.springerlink.com/content/m8l86l8n3h81w43m/

7. ten Tusscher KHWJ, Panfilov AV. Alternans and spiral breakup in a human ventricular tissue model. Am. J. Physiol. Heart Circ. Physiol. 2006 Sep;291(3):H1088–1100.

8. Rice JJ, Wang F, Bers DM, de Tombe PP. Approximate model of cooperative activation and crossbridge cycling in cardiac muscle using ordinary differential equations. Biophys. J. 2008 Sep;95(5):2368–90.

9. Adeniran I, McPate MJW, Witchel HJ, Hancox JC, Zhang H. Increased Vulnerability of Human Ventricle to Re-entrant Excitation in hERG-linked Variant 1 Short QT Syndrome. Plos Comput Biol. 2011;

10. Silva J, Rudy Y. Subunit interaction determines IKs participation in cardiac repolarization and repolarization reserve. Circulation. 2005 Sep 6;112(10):1384–91.

11. Adeniran I, El Harchi A, Hancox JC, Zhang H. Proarrhythmia in KCNJ2-linked short QT syndrome - insights from modelling. Cardiovascular Research. 2012;